minerals

MDPI

Article

Reservoir Characteristics and Controlling Factors of Large-Scale Mono-Block Gas Field Developed in Delta-Front Sandstone—A Case Study from Zhongqiu 1 Gas Field in the Tarim Basin

Songbai Zhu [1], Quanwei Du [2], Chen Dong [1], Xue Yan [1], Yong Wang [1], Yanli Wang [1], Zhuangsheng Wang [3] and Xiaobing Lin [3,*]

1 Tarim Oilfield, PetroChina, Korla 841000, China; zsbai-tlm@petrochina.com.cn (S.Z.); dongchen-tlm@petrochina.com.cn (C.D.); yanxue-tlm@petrochina.com.cn (X.Y.); wwangy1-tlm@petrochina.com.cn (Y.W.); wyanl-tlm@petrochina.com.cn (Y.W.)
2 PetroChina Oil, Gas, and New Energy Branch, Beijing 100007, China; duquanwei@petrochina.com.cn
3 Institute of Sedimentary Geology, Chengdu University of Technology, Chengdu 610059, China; 19980830820@163.com
* Correspondence: linxiaobing07@cdut.edu.cn

Abstract: Taking the Zhongqiu 1 Gas Field in the Tarim Basin as an example, the heterogeneity of large-scale mono-block gas fields and their primary controlling factors have been analyzed. Based on drilling core data, well log data, scanning electron microscopy, thin-section analysis, and mercury injection experiments, combining sedimentological interpretation, research on the reservoir characteristics and variability was carried out. The results showed that: (1) The lithologic characteristics showed obvious variations among wells in the Zhongqiu 1 gas field. Specifically, the main lithology developed in the Zhongqiu 1 well is feldspar lithic sandstone, while the remaining wells predominantly consist of lithic feldspar sandstone. These differences in rock composition maturity reveal that a higher proportion of stable mineral components leads to poorer reservoir properties; (2) the main factors controlling oil and gas productivity include the variations in petrology, mineralogy, and diagenetic process characteristics. The high content of unstable mineral components and constructive diagenesis could increase reservoir porosity together. (3) Sedimentary facies of the Bashijiqike Formation in the Zhongqiu 1 Gas Field played a dominant role in the reservoir distribution. The division of sedimentary facies zones reflects variations in material composition and grain size, serving as the main material basis for reservoirs. Differences in mineral composition reflect the sedimentary environment of the reservoir. Additionally, mineral composition indicates the relationship between diagenetic processes and reservoir evolution. The high feldspar content in well ZQ1 corresponded to relatively favorable reservoir properties. The dominant feldspar type was plagioclase, suggesting that early-stage chemical weathering had undergone significant alteration. The above conclusions provided a microscopic perspective to explain the differences in oil and gas production capacity of large delta-front gas fields, serving as a geological basis for the exploration and exploitation of similar fields.

Keywords: reservoir capabilities; rock composition; diagenesis; sedimentary facies; reservoir pore space

check for updates

Citation: Zhu, S.; Du, Q.; Dong, C.; Yan, X.; Wang, Y.; Wang, Y.; Wang, Z.; Lin, X. Reservoir Characteristics and Controlling Factors of Large-Scale Mono-Block Gas Field Developed in Delta-Front Sandstone—A Case Study from Zhongqiu 1 Gas Field in the Tarim Basin. *Minerals* **2023**, *13*, 1326. https://doi.org/10.3390/min13101326

Academic Editor: Santanu Banerjee

Received: 20 September 2023
Revised: 11 October 2023
Accepted: 12 October 2023
Published: 13 October 2023

Copyright: © 2023 by the authors. Licensee MDPI, Basel, Switzerland. This article is an open access article distributed under the terms and conditions of the Creative Commons Attribution (CC BY) license (https://creativecommons.org/licenses/by/4.0/).

1. Introduction

The Qiulitag tectonic zone in the Kuqa depression is a sliding backslope tectonic structure with favorable conditions for both tectonic activity and hydrocarbon formation. The Jurassic humus-type coal series source rocks are the main hydrocarbon source layers [1–3]. The late Himalayan tectonic activities have formed large wedge-shaped structures, providing excellent reservoir layers. The thick salt rocks from the Paleogene and Neogene periods serve as excellent cap rocks. The fulfillment of these conditions ensures a favorable temporal and spatial match for hydrocarbon generation and trap formation in the Qiulitag structural belt [1–3]. Large and medium-sized condensate reservoirs, such as Dina, Dongqiu, Zhongqiu, etc., have also been discovered [1–4]. However, variations in oil and gas production capacity gradually appeared during the deepening progress of exploration and exploitation. Further research is needed on the structural evolution, sedimentary sequence, formation laws of strata and reservoirs, and productivity control factors [5–10].

The Zhongqiu 1 Gas field, located in the eastern section of the Qiulitag tectonic zone in the northern part of the Kuqa depression, is a mono-blocky, anticline-type, normal-temperature, ultra-high-pressure, low-condensate-containing condensate gas field with a wide and gentle anticline (Figure 1d). The dense sandstone reservoir is the main reservoir of the Cretaceous Bajiqike Formation. Jurassic humic coal is the main source rock. The Zhongqiu 1 Gas field has been explored and developed since 2018, with over ten billion cubic meters of proven gas condensate reserves [4]. Among them, the ZQ1 well was completed in 2018 and achieved positive oil testing results in the Cretaceous Bashijiqike Formation, with daily gas production of more than 500 thousand cubic meters. The daily gas production of wells ZQ11, ZQ12, and ZQ2, which were subsequently drilled and put into operation, is less than 100 thousand cubic meters, with a significant difference in production capacity compared to the ZQ1 well.

Previous research concluded that the thick, Cretaceous sandstone stratum of the Zhongqiu 1 Gas field belongs to the front edge of the braided river delta, with characteristics of abrupt lateral changes in sedimentary facies [4,11,12]. The main lithology is lithic feldspathic sandstone and feldspathic lithic sandstone [12,13]. The pore type is dominated by primary intergranular pores, and the fracture is underdeveloped, making it a typical pore-type reservoir [2–4,9,11,12]. Therefore, the difference in production capacity between wells in the same gas field is not only affected by development measures but also by geological conditions. On the basis of previous research, in this study, we collect and analyze drilling data, core data, logging data, field profile data, and productivity data of the Zhongqiu 1 Gas field. Studying the characteristics and differences between reservoirs reveals their main controlling factors. The distribution pattern of high-quality reservoirs was predicted, providing a basis for further exploration and development of large-scale sandstone gas fields in the delta front.

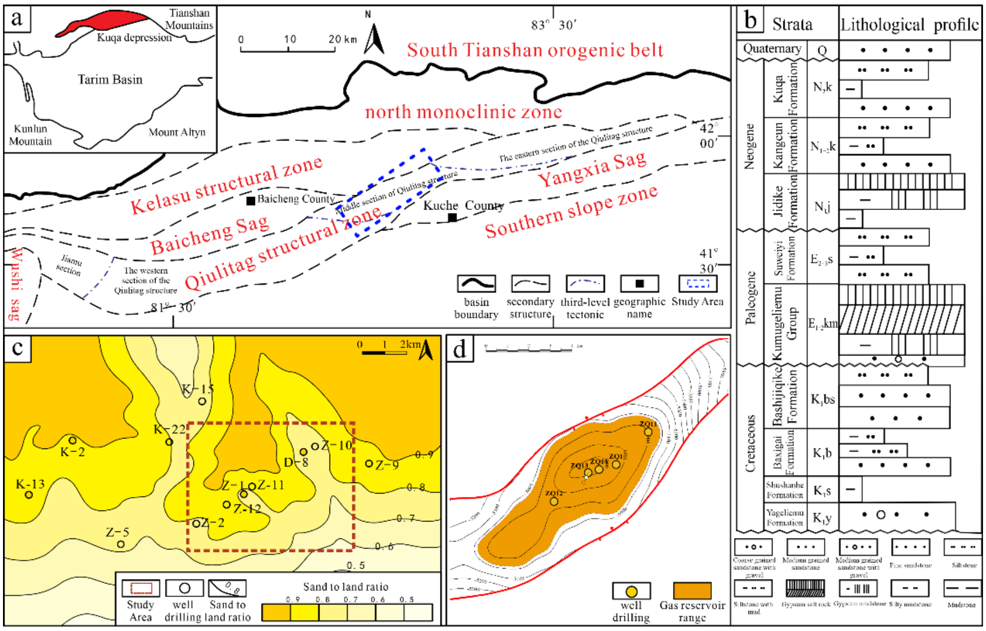

Figure 1. Structural geological background of the study area. (**a**). Tectonic location map of the study area (According to [13] revised); (**b**). Comprehensive stratigraphic column of the study area

(According to [13] revised); (**c**). Contour map of the sand-to-land ratio of the study area (provided by Kela Oil and Gas Production Management Zone of PetroChina Tarim Oilfield Branch, sand-to-land ratio is equal to the ratio of pure sandstone thickness to formation thickness); (**d**). Tectonic map of the Zhongqiu 1 gas fields (According to [13] revised).

2. Geological Setting

The Kuqa depression, situated at the northern periphery of the Tarim Basin, has witnessed a sequence of significant tectonic events spanning three main stages. Initially, during the Hercynian orogeny at the conclusion of the Late Paleozoic era, the entire Kuqa region experienced substantial extrusion and deformation. This was followed by the Yanshan tectonic movement in the Late Jurassic period, characterized by intense uplift resulting in stratigraphic erosion and the establishment of unconformable contacts between the Jurassic and Cretaceous formations [11,12].

Subsequently, the Cenozoic Xishan movement exerted strong north–south compression forces, leading to the contraction and deformation of the Kuqa area. Following multiple superimposed tectonic movements and transformations, this complex geological history culminated in the development of the present "four belts, three concave, and one rift" tectonic pattern. Specifically, the Qiulitag tectonic belt occupies the southern sector of the Kuqa depression, further divided into four secondary tectonic units: the eastern Jiamu section, the Xiqiu section, the eastern Zhongqiu section, and the Dongqiu section. The focus of this study is situated within the Zhongqiu section [2,11,12] (Figure 1a).

As a result of Late Cretaceous tectonic uplift in the Southern Tien Shan region, the Upper Cretaceous strata in the study area underwent denudation, leaving only the Lower Cretaceous strata intact. These Lower Cretaceous formations are characterized by angular unconformities with the overlying Paleocene Kumgelimu group and disconformities with the underlying Upper Jurassic Kazhala Formation. The Lower Cretaceous sequence comprises, from bottom to top, the Yageliemu Formation (K_1y), the Shushanhe Formation (K_1s), the Baxigai Formation (K_1b), and the Bashijiqike Formation (K_1bs). The lithology of the Bashijiqike Formation is predominantly fine sandstone, forming a favorable reservoir cap association with the overlying gypsum salt rock strata of the Kumugeliemu group ($E_{1–2}$ *km*) (Figure 1b).

The primary reservoir section within the study area is the Cretaceous Bashijiqike Formation, further subdivided into two lithological sections, namely the K_1bs^1 section and the K_1bs^2 section, arranged from top to bottom. The K_1bs^2 formations are further divided into three sandstone section: Section 1 (K_1bs^{2-1}), Section 2 (K_1bs^{2-2}), and Section 3 (K_1bs^{2-3}).

The Cretaceous Bashijiqike Formation of the Kuqa depression is primarily characterized by deposition in a braided river deltaic environment. These sediments were predominantly sourced from the southern slopes of the Tian Shan Mountains [3,14] (Figure 1c). The primary factor contributing to the deposition of these exceptionally thick sedimentary rock layers is the extensive tectonic subsidence that has occurred from the Mesozoic to the Cenozoic era. This subsidence is a far-field response to the collision and compression between the Indian Plate and the Asian Plate [3,14] (Figure 1c).

3. Materials and Methods

Data from four wells in the Zhongqiu area were obtained (Figure 1d). The drilling lithology logs, logging curve data, and physical property data were provided by the Kara Oil and Gas Production Management Area of the Tarim Oilfield Branch of the China National Petroleum Corporation. Information from thin sections, scanning electron microscopic data, and high-pressure mercury pressure data were analyzed and obtained by the State Key Laboratory of Oil and Gas fields of Chengdu University of Technology.

The logging data included Gamma-Ray (GR), KTH gamma-ray without uranium (KTH), and resistivity curves (including M2R3, M2R6, and M2RX curves) provided by the logging database of the PetroChina Tarim Oilfield Branch. Logging data were depthcorrected on the basis of the core section of the Bashijiqike Formation. A total of 853.1 m lithological log corrections were completed, including GR, KTH, M2R3, M2R6, and M2RX log curves. The spacing of the interpretation points was set at 0.125 m. The log data were processed using ResFrom GeoOffice v3.5 software developed by Kaben. Outliers were removed by correcting the depth of the logs.

Rock flakes were sampled and produced under the license of PetroChina Tarim Oilfield Branch at 1 m intervals, and the longitudinal cores were cut using an SYJ-200 fully automatic precision cutting machine. Common thin sections were ground by a UNIPOL-1202 automatic precision grinder; then, the ground samples were polished using a GPC-80A precision grinding and polishing control instrument. The thin section was die-cast using a plexiglass monomer casting method. The coloring material was blue methyl methacrylate monomer solution, and the resin-filling and glass-covering operations were completed using an MTI-3040 heating table and a DZF-6020 vacuum drying oven. Rock flake identification was carried out at the Institute of Sedimentary Geology, Chengdu University of Technology, using an optical microscope (Nikon E600 POL, Tokyo, Japan) according to the "Technical Specification for Rock and Mineral Identification of the Geological and Mineralogical Industry Standard of the People's Republic of China", DZ/T0275.1-2015. A total of 192 common thin sections and 111 cast thin sections were prepared and identified, and SEM was carried out according to the SY/T 5162-2014 standard using a Quanta200 SEM and an EDAX spectrometer with a maximum resolution of 1.4 nm and magnification of 50×~3450× and a total of 102 SEM images identified.

Data on physical properties were provided by the Quality Inspection Centre of PetroChina Tarim Oilfield Branch based on core analysis method GB/T 29172-2012. The porosity and permeability were determined using a ZYB-IB vacuum-pressurized saturator, a liquid densitometer, a gas densitometer, and an AL204 electronic balance, with the physical properties determined for a total of 340 samples.

Utilizing the aforementioned dataset, an extensive analysis of the primary attributes and distinctions among reservoirs within the study area was conducted. This analysis encompassed the detailed characterization and classification of reservoir rock types. Furthermore, the physical properties of the reservoirs were meticulously examined, facilitating the identification and categorization of primary reservoir storage space types. By considering the disparities among various reservoir factors, a comprehensive assessment of the key controlling elements was undertaken. Subsequently, the establishment of prediction criteria for high-quality reservoirs based on these primary controlling factors was executed. This endeavor was undertaken with the overarching objective of providing a geological foundation to support the exploration and development of large-scale delta-front sandstone-type gas fields.

4. Results

4.1. Petrological and Mineralogical Characteristics of Reservoirs

Based on the thin section analysis of core samples from four wells within the gas field, the primary rock types identified in the Zhongqiu 1 Gas field are feldspar lithic sandstone and lithic sandstone. Notably, there are distinct variations in drilling lithology among these wells. Specifically, the ZQ1 well is predominantly composed of feldspar lithic sandstone, while the ZQ11, ZQ12, and ZQ2 wells exhibit a prevailing lithic feldspar sandstone composition (Figure 2a). Furthermore, an observed trend reveals a gradual increase in the proportions of quartz and feldspar in the ZQ1, ZQ11, ZQ12, and ZQ2 wells, accompanied by a corresponding decrease in rock fragment content (Figure 2c).

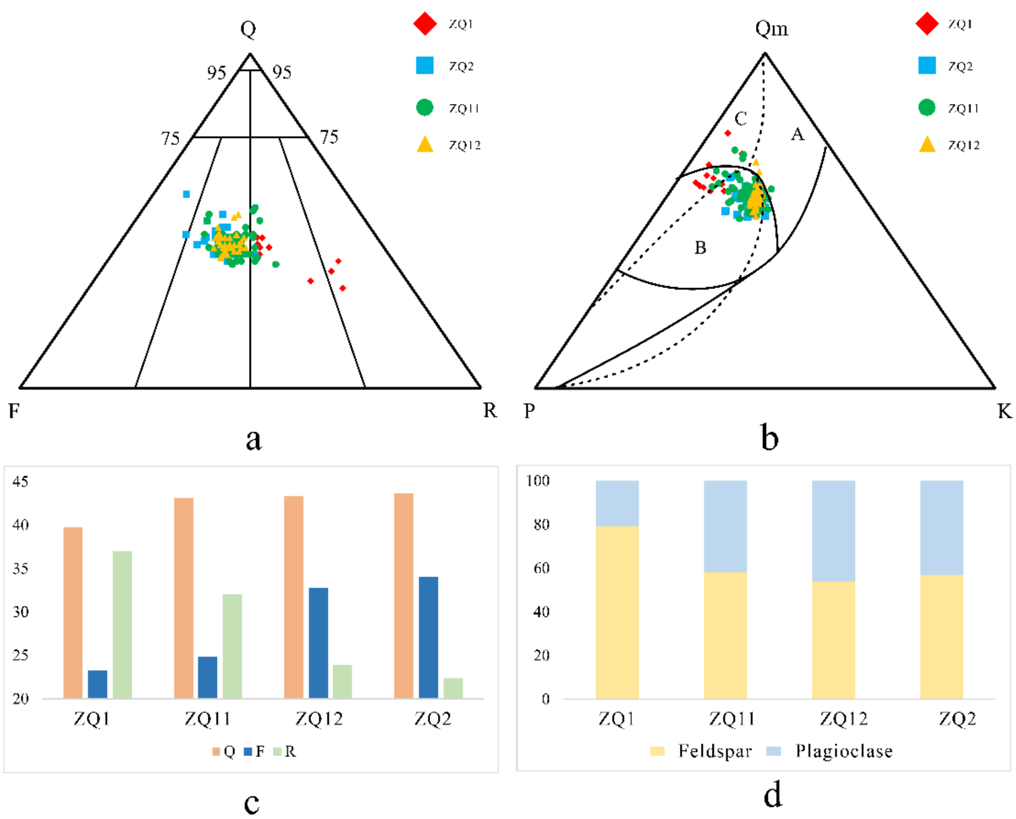

Figure 2. Reservoir rock types. (**a**). Triangular diagram of the rock types in the reservoir of the Zhongqiu 1 gas field; (**b**). Dickinson diagram of Zhongqiu 1 gas field (A—sources from stable continental plates; B—Sources from volcanic island arcs; C- Sources from orogenic belts); (**c**). Histogram of the average content of major particles in the Zhongqiu 1 field. (**d**). Potassium feldspar plagioclase ratio bar chart of Zhongqiu 1 gas field; significance of symbols: Q-quartz; F: feldspar; R: rock fragments.

Through thin-section observations and identifications, the particle composition and content of the Bashijiqike Formation in the Zhongqiu 1 Gas field were statistically analyzed. Utilizing the Dickinson diagram, it was determined that the provenance of lithic fragments in the Zhongqiu 1 well primarily originated from a re-circulating orogenic belt source area. In contrast, the ZQ11, ZQ12, and ZQ2 wells were primarily associated with a magmatic island arc provenance, with an increasing ratio of plutonic and volcanic rock sources. Notably, some samples from the ZQ12 well were found to be within a stable continental block provenance area (Figure 2b).

These findings indicate a disparity in provenance areas between the ZQ1 well and the other wells in the Zhongqiu field, with the ZQ11 and ZQ2 wells exhibiting a broader range of provenance sources, while the ZQ12 well displays a more concentrated source area.

The ZQ1 well consistently exhibits lower average quartz content compared to the ZQ11, ZQ12, and ZQ2 wells (Figures 2c and 3). In contrast, the feldspar content gradually increases while the lithic fragment content gradually decreases, indicating characteristics of relatively short-distance transportation. Potassium feldspar dominates the feldspar composition in the ZQ1 well, with a relatively small proportion of plagioclase feldspar (Figure 2d). In contrast, the other three wells display less disparity in the proportions of these two types of feldspar. The presence of plagioclase feldspar suggests an early stage of chemical weathering [15], implying a comparatively higher degree of chemical weathering in the ZQ1 well relative to the other three wells.

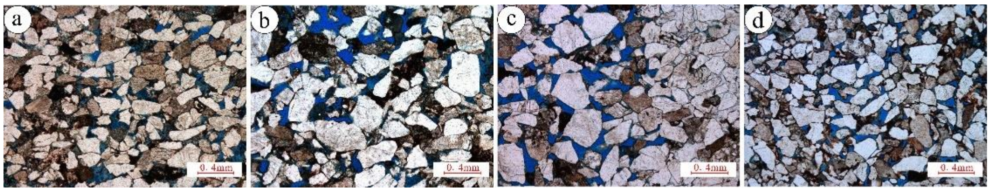

Figure 3. (**a**). ZQ1 well, 6075.3 m; (**b**). ZQ11 well, 6330.6 m; (**c**). ZQ12 well, 6215.0 m; (**d**). ZQ2 well, 6331.6 m.

4.2. Reservoir Physical Characteristics

Obvious differences can be observed in the physical properties among the wells drilled in the Zhongqiu 1 Gas field. The porosity of the Bashijiqike Formation in the ZQ 11, ZQ12, and ZQ2 wells ranges from 1.17% to 16.40%, with an average value of 10.18% and a peak interval of 10% to 12% (Figure 4a). The permeability ranges from 0.0458 to 9.17 mD, with an average value of 18.69 mD and a peak interval of 1.0 to 4.0 mD (Figure 4b). The reservoir porosity values of the ZQ11 and ZQ12 wells do not differ considerably, with peak porosity distribution ranging from 10% to 16% (Figure 4c). The peak interval of reservoir porosity distribution in the ZQ2 well is 8%~12% (Figure 4c). The permeability of the ZQ2 and ZQ12 wells is predominantly low, but the extra-low permeability of the ZQ2 well is greater than that of the ZQ12 well (Figure 4d). The peak permeability of the ZQ2 well ranges from 1 to 4 mD, and the peak permeability of the ZQ12 well is greater than 4 mD (Figure 4d).

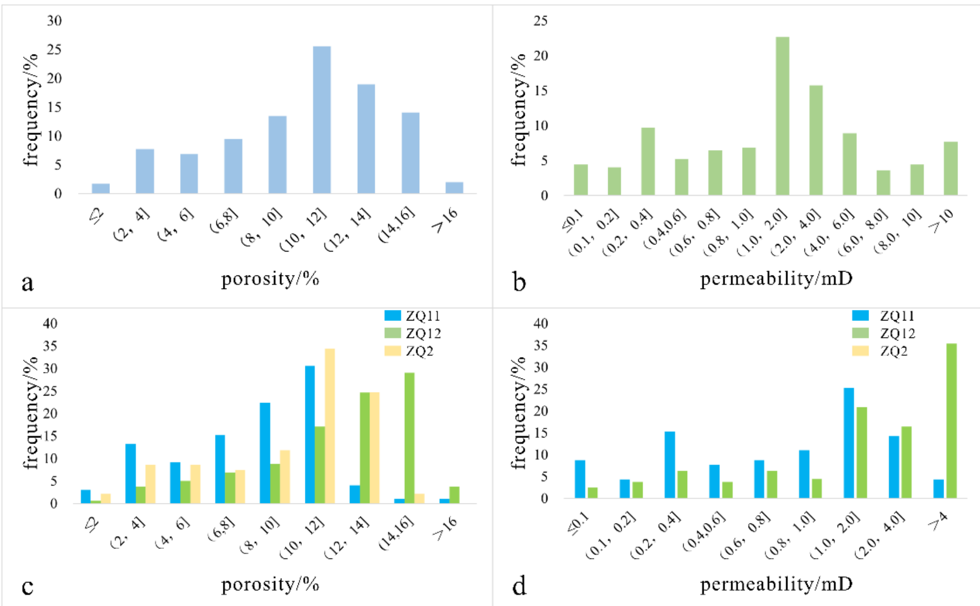

Figure 4. Physical characteristics of the Bashijiqike Formation in the Zhongqiu 1 gas field. (**a**). Histogram of the frequency of distribution of measured porosity in the core of the Zhongqiu 1 gas field; (**b**). Histogram of the frequency of distribution of measured permeability in the core of the Zhongqiu 1 gas field; (**c**). Histogram of the frequency of distribution of measured porosity in the core of each well; (**d**). Histogram of the frequency of distribution of measured permeability in the core of each well reservoir rock types.

4.3. Reservoir Space Type and Plane Porosity

The reservoir storage space within the Bashijiqike Formation of the Zhongqiu 1 Gas field can be categorized into two primary types: pores and cracks. Pores exhibit a higher level of development and are predominantly characterized by primary intergranular pores, residual primary intergranular pores, and intergranular dissolution pores. Additionally, a smaller quantity of intragranular dissolution pores is observed. In contrast, cracks mainly manifest as contraction cracks, with occasional occurrences of tectonic cracks and dissolution cracks (Table 1 and Figure 5).

Table 1. Statistical table of plane porosity of different reservoir space types in Zhongqiu field.

Well	Layer	Number of Samples	(Residual) Primary Intergranular Pores	Intergranular Dissolved Pore	Intragranular Dissolved Pore	Micro-Pores	Crack	Total Plane Porosity
ZQ1 well	K_1bs^1	8	1.9~6.0% 3.7%	1.1~5.0% 2.5%	0.1~0.5% 0.3%	0.8~2.5% 2.1%	0~0.5% 0.31%	3.2~7.2% 5.5%
	K_1bs^2	8	3.6~14.0% 9.1%	2.3~5.0% 3.5%	0.1~0.5% 0.3%	0~0.5% 0.2%	0~0.4% 0.27%	5.1~19.4% 13.0%
ZQ11 well	K_1bs^1	27	0.3~13.6% 5.4%	0~1% 0.3%	0~0.5% 0.27%	0~0.5% 0.26%	0~0.3% 0.2%	0.4~14.7% 6.0%
	K_1bs^2	15	4.0~10.0% 6.2%	0~0.8% 0.3%	0~0.3% 0.16%	0~0.3% 0.14%	/ /	4.7~10.4% 6.7%
ZQ12 well	K_1bs^1	20	0.1~8.5% 4.1%	0~0.8% 0.35%	0~0.1% 0.02%	0~0.5% 0.28%	0~0.5% 0.025%	0.1~9.0% 4.7%
	K_1bs^2	6	1~12% 4.75%	0~0.5% 0.3%	/ /	/ /	/ /	1~12.5% 4.96%
ZQ2 well	K_1bs^1	19	0.3~4% 2.2%	0~0.3% 0.14%	0~0.2% 0.025%	0~0.2% 0.4%	0~0.2% 0.075%	1~5.5% 2.37%
	K_1bs^2	9	0.5~8.3% 4.9%	0~0.4% 0.15%	0~0.2% 0.03%	0~0.2% 0.07%	/ /	1~9.2% 5.3%

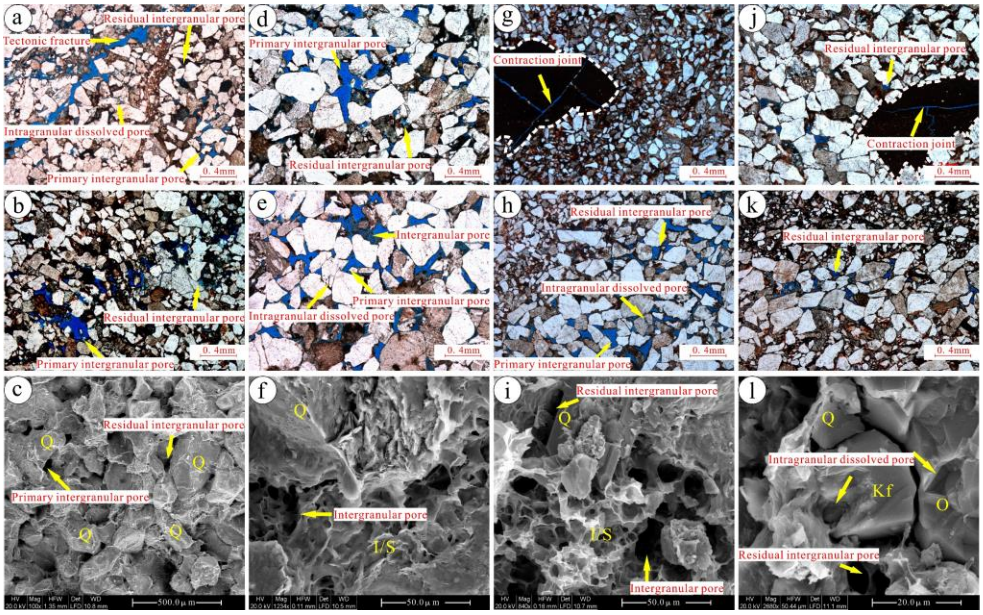

Figure 5. Pore types in Zhongqiu field. (**a**). ZQ1 well, 6076.0 m; (**b**). ZQ1 well, 6160.0 m; (**c**). ZQ1 well, 6163.5 m (×100); (**d**). ZQ11 well.6330.7 m; (**e**). ZQ11 well, 6336.4 m; (**f**). ZQ11 well, 6299.33 m (×1234); (**g**). ZQ12 well, 6208.87 m; (**h**). ZQ12 well, 6214.95 m; (**i**). ZQ12 well, 6214.95 m (×840); (**j**). ZQ2 well, 6332.06 m; (**k**). ZQ2 well, 6335.76 m; (**l**). ZQ2 well, 6330.22 m (×2680).

In the Zhongqiu field, the prevailing pore types comprise primary intergranular pores and residual primary intergranular pores (Figure 5a,c–e,h). Primary intergranular pores exhibit well-defined boundaries and remain unobstructed by gap fillers, as evident in Figure 5d,e. In contrast, residual primary intergranular pores are filled with gap fillers and are predominantly characterized by an argillaceous matrix, as well as calcite and gypsum cementation (Figure 5a,b,h,k).

Secondary pores comprise both intergranular and intragranular pores (Figure 5a,b,h,k). Intergranular dissolved pores originate from the dissolution of interstitial material between grains, and residual interstitial components are discernible. The boundaries of these pores exhibit irregular or serrated features (Figure 5d,e,i). Intragranular pores are a product of feldspar and clast dissolution, characterized by a shallow degree of particle dissolution, intact boundaries, and predominantly centralized dissolution patterns, with occasional dissolution occurring along joints (Figure 5a,e,h,l). The dissolution of debris or clay minerals results in the formation of a honeycomb-like structure, which is observable in Figure 5f,i. Secondary porosity constitutes approximately 30% of the total porosity in the ZQ1 well, while it ranges from 2% to 7% in the remaining three wells.

Shrinkage joints in mud clasts, structural microcracks, and dissolution fractures can be identified in rock thin sections. The most common type of microcrack is the shrinkage joint within mud clasts. Rocks undergo the influence of pressure and temperature from overlying strata during burial, causing trapped water within the muddy matrix to gradually precipitate. This process results in the contraction of mud clasts and fine-grained fill materials, forming microcracks that typically extend only through the mud clasts and remain devoid of any filling material. Structural fractures are less common but may be filled with calcite and gypsum (Figure 5a,g,j).

The total planar porosity in well ZQ1 is higher than that in the other three wells. In ZQ1, the (residual) primary intergranular pores account for over 60% of the total planar porosity, while intergranular and intragranular pores collectively constitute approximately 35% of the total planar porosity. Fractures contribute to around 4% of the total planar porosity, whereas the muddy micro-pore space comprises a relatively small portion of the planar porosity (typically less than 1%). In contrast, the reservoir space in wells ZQ11, ZQ12, and ZQ2 is primarily composed of primary intergranular pores and residual primary intergranular pores, accounting for over 90% of the total planar porosity (Figure 6a,b).

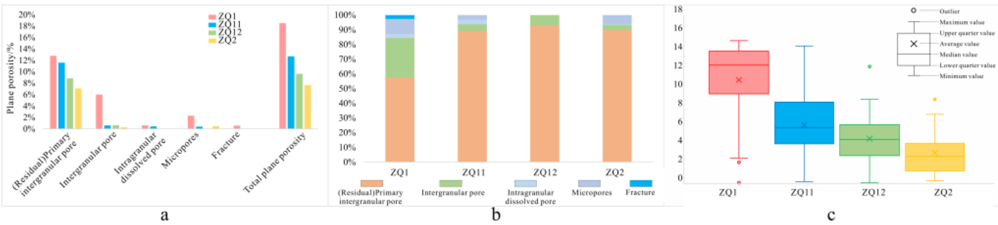

Figure 6. Zhongqiu field face rate characteristics. (**a**). Percentage of reservoir space type plane porosity rate; (**b**). Percentage of each well reservoir space type; (**c**). Plane porosity Box Figure.

An analysis of the porosity values in the Zhongqiu field, conducted using box plots, reveals distinct patterns. Specifically, in well ZQ1, the porosity distribution exhibits a relatively wide range, with a predominant concentration of high values. The average and median values in ZQ1 are notably higher than those in the other three wells, with occasional occurrences of low outliers. This suggests an overall higher porosity in ZQ1, characterized by a diverse range of pore types and relatively elevated porosity levels.

Conversely, wells ZQ101, ZQ102, and ZQ2 display porosity distributions that are predominantly concentrated in the low-value range. Their average, median, as well as upper and lower quartile values, are comparatively lower. Occasionally, there are outliers indicating exceptionally high porosity values. This pattern suggests a more uniform pore type with lower overall porosity levels in these wells (Figure 6c).

5. Discussion

The Zhongqiu 1 Gas field, located within the Bashijiqike Formation, received sedimentary materials from the southern part of the Tian Shan Mountains and was primarily deposited in a proximal deltaic sedimentary environment. Subsequently, it underwent an overburdened burial phase [16–19]. This reservoir exhibits multiple controlling factors, among which sedimentary environment [20–22] and diagenesis [23–28] are the primary drivers of reservoir property variations [13,29,30].

5.1. The Influence of Sedimentary Facies and Mineral Composition on Reservoir Characteristics

The Zhongqiu field primarily exhibits the braided river delta-front subphase, characterized by the prevalence of distributary channel, mouth bar, and interdistributary bay facies. The dominant sand bodies in this region consist of distributary channel sand bodies and mouth bar sand bodies, as illustrated in Figure 7 [15] (Figure 7).

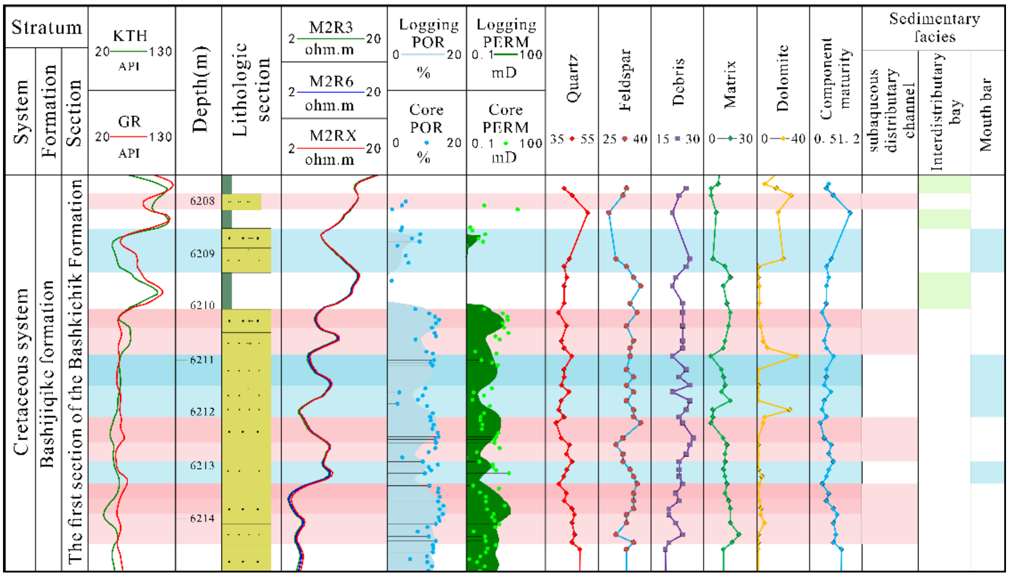

Figure 7. The influence of sedimentary facies and mineral composition on reservoir properties.

The sedimentary features of the distributary channel microphase, including both the grain sequence (as evidenced by the GR curve) and the sand body (as indicated by the KTH curve), prominently exhibit a box and bell shape. Concurrently, the resistivity curve consistently indicates low values, signifying a relatively low mud content [31]. Additionally, there is a gradual decrease in the content of quartz particles from the base to the top of the sequence, while the feldspar content exhibits an ascending trend. Although the variation in rock fragment content is less pronounced, the composition maturity gradually declines, accompanied by an increase in mud content. Regarding grain size, the sand body becomes progressively finer, and the rock core initially experiences an increase followed by a decrease in both porosity and permeability within the middle and lower sections of the river channel sand body.

Both the upper and lower boundaries of the river channel sand body feature scouring surfaces. Within the mouth bar microphase sedimentary sequence, the sand body primarily assumes a funnel-shaped grain sequence (as evidenced by the GR curve and KTH curve) and is accompanied by a high-resistivity curve. The content of quartz particles gradually diminishes, while the feldspar content exhibits a progressive increase, and the composition maturity experiences a gradual rise. The porosity of the rock core initially decreases, followed by an increase.

In high-quality reservoirs, sand bodies within distinct sedimentary facies undergo varying physical alterations across different regions [22,32]. At the leading edge of the submerged braided river delta, the erosive impact of the river diminishes significantly. During this phase, wave action assumes a predominant role in reshaping sedimentary sand bodies. This phase is characterized by microphase transitions and abrupt compaction. Factors contributing to the differential distribution of reservoirs primarily include reduced preservation of intact channel sands and mouth bar sands, as well as frequent cutting and stacking processes [33–36].

Mineral content is also a primary influencing factor on reservoir properties. Feldspar exhibits high solubility, and in Figure 8, it can be observed that intervals with higher feldspar content tend to have relatively better reservoir properties. Additionally, calcite is the primary filler material; hence, a higher content of calcite indicates that the pore spaces are filled, leading to reduced porosity and permeability. Composition maturity represents the ratio of stable mineral content (such as quartz) to relatively unstable mineral content (such as feldspar and debris). A higher composition maturity signifies a higher proportion of stable minerals, resulting in relatively smaller reservoir spaces (Figure 7).

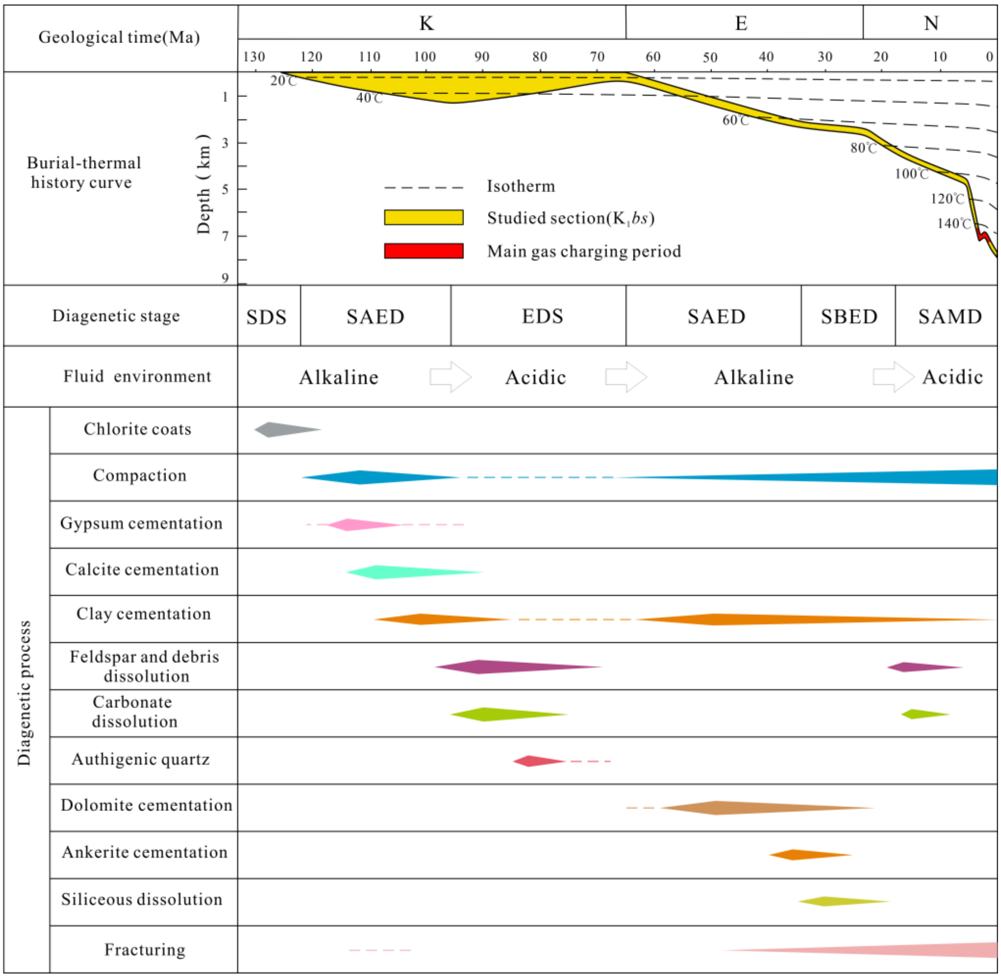

Figure 8. Diagenetic sequence diagram of Zhongqiu 1 gas reservoir. SDS = Syndiagenetic Stage; SAED = Stage A of Early Diagenesis; EDS = Epodiagenetic Stage; SBED = Stage B of Early Diagenesis; SAMD = Stage A of Middle Diagenesis.

5.2. The Control of Diagenesis on Reservoir Quality

The diagenesis of sandstone reservoirs in the Zhongqiu area of the Qiulitag tectonic belt, situated within the Kuqa depression of the Tarim Basin, demonstrates a multifaceted character. This process encompasses a range of diagenetic phenomena, including compaction, pressure solution, cementation, dissolution, metasomatism, and fracturing [37–40].

Utilizing techniques including rock thin sections and scanning electron microscopy, we established the diagenetic timing and stages of the Zhongqiu 1 Gas field. A diagenetic sequence map for the Zhongqiu 1 Gas field was then meticulously crafted (Figure 8).

5.2.1. Diagenetic Compaction Processes Diminish Reservoir Space

Compaction diagenesis occurs throughout the burial history, and strong compaction is one of the main reasons for the abrupt reduction in pore space in the early diagenetic stage [14,41,42]. In addition, compaction can squeeze the heterogeneous clay base into a pore throat, which can disrupt the connectivity of the pore-throat channel. Cementation also fields the pore throat, reducing the pore space [43,44].

The Zhongqiu section of the Qiulitag tectonic zone, situated within the Kuqa depression, experiences a substantial burial depth exceeding 6000 m. Consequently, the sandstone reservoirs in this region undergo significant compaction, resulting in the formation of linear or concave–convex contacts between particles (Figure 9a,c). Plastic particles undergo extrusion and deformation during this process (Figure 9a). Furthermore, as certain rigid particles bear increasing pressure, they may rupture under intense force (Figure 9b), leading to dissolution phenomena along the resultant cracks. As the burial depth continues to rise, both pressure and temperature within the sandstone increase, rendering the quartz grains less stable. The pressure–solution effect causes some quartz grains to come into contact with each other through sutures (Figure 9c). The relatively poor sorting in the sandstone allows particles of varying sizes to coexist, with larger particles seemingly providing additional support and thereby preserving more primary polygonal pores (Figure 9a) [28,45].

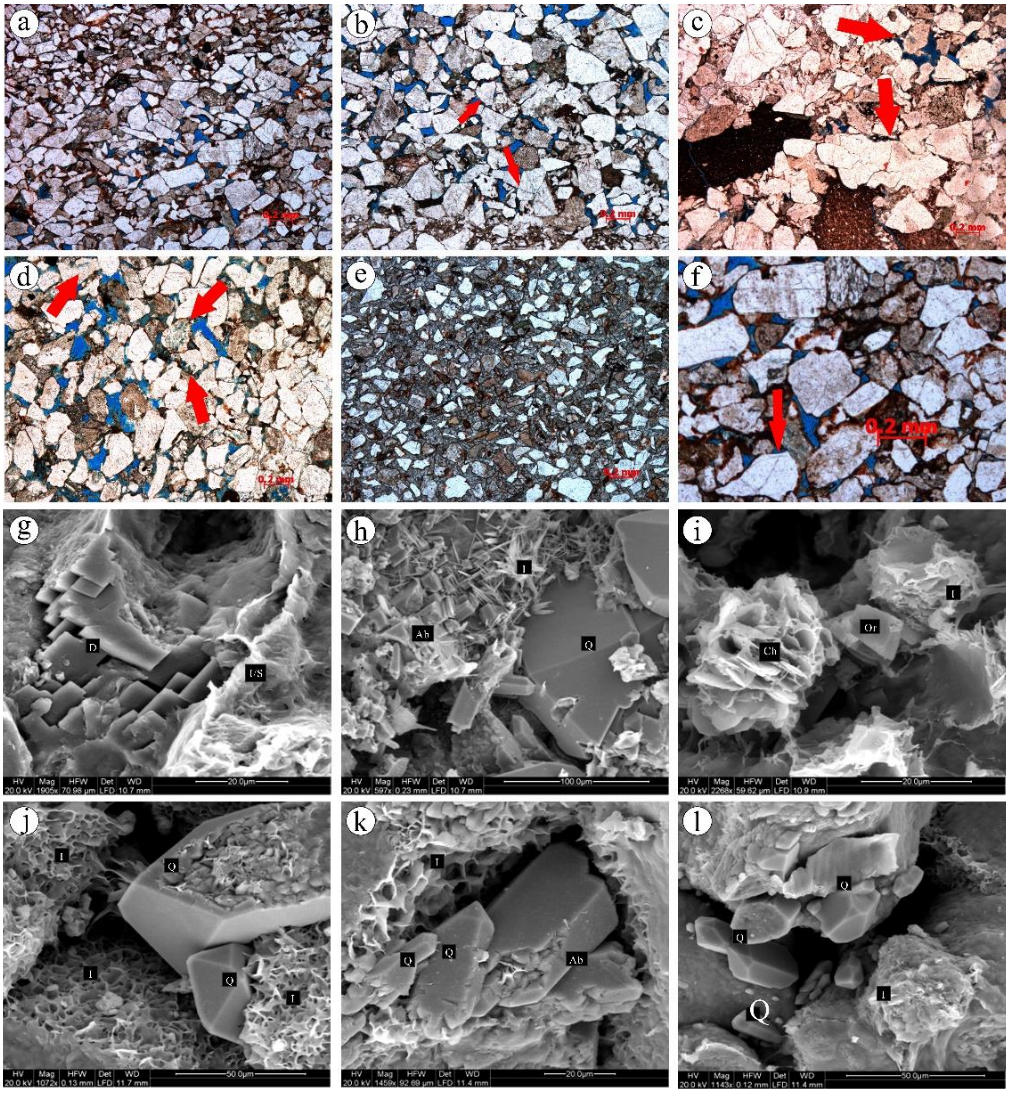

Figure 9. Diagenesis in Zhongqiu field. (**a**). ZQ2 well, 6327.57 m, single polarized; (**b**). ZQ2 well, 6425.03 m, single polarized; (**c**). ZQ11 well, 6294.88 m, single polarized; (**d**). ZQ11 well, 6288.3 m, single polarized; (**e**). ZQ2 well, 6334.12 m, single polarized; (**f**). ZQ2 well, 6327.57 m, single polarized; (**g**). ZQ2 well, 6328.03 m, single polarized; (**h**). ZQ2 well, 6423.57 m; (**i**). ZQ11 well, 6332.74 m; (**j**). ZQ11 well, 6298.19 m; (**k**). ZQ11 well, 6285.10 m; (**l**). ZQ12 well, 6391.85 m.

5.2.2. The Original Intergranular Pores were Destroyed by Cementation

The primary cementation types within the reservoirs in the study area encompass carbonate cementation, siliceous cementation, and argillaceous cementation. Dolomite serves as the primary cement in the sandstone reservoirs, and it is abundantly observed under the microscope in the form of grain mosaic and basal cementation (Figure 9e), leading to reduced pore space development. Siliceous cementation predominantly manifests as secondary quartz enlargement (Figure 9f), often composed primarily of chlorite. Small authigenic quartz grains can be observed within the interstitial pores among grains (Figure 9l). Anhydrite cementation is relatively less pronounced and occurs as cemented hyaline patches (Figure 9d). Residual montmorillonite is evident at the dissolution margins of feldspar grains, while a mixed illite–montmorillonite layer frequently appears as an intermediate phase during the transformation from montmorillonite to illite, typically in a honeycomb or cottony form (Figure 9g). Illite fills the intergranular spaces in filamentous or acicular forms (Figure 9h,j), with chlorite coating the grain surfaces in a thin layer (Figure 9i).

5.2.3. Dissolution Increases the Volume of Reservoir Space

Dissolution and erosion processes play a substantial role in modifying reservoir porosity [45]. Alongside the pronounced extrusion associated with Xishan tectonic movement, the sandstone in this region experienced the development of numerous tectonic fractures. These fractures can facilitate the favorable migration of oil and gas [5,6,9]. Throughout the evolutionary process of rock formation, the origin and composition of rock-forming fluids are multifaceted, resulting in a diversity of dissolution mechanisms [46,47].

Under acidic conditions, feldspars, debris, and carbonate minerals undergo destabilization. This results in the exposure of eroding particle edges, with some particles partially covered by erosion residue. Intergranular erosion holes are formed, and intragranular erosion holes are also prevalent (Figure 9c,d). Scanning electron microscopy reveals the dissolution of dolomite grain edges (Figure 9g), albite dissolution (Figure 9k), and illite filling at the dissolved edges of potassium feldspar (Figure 9i). In alkaline environments, quartz is susceptible to dissolution, and some microscopic quartz grains can be observed with irregular concavities or recesses along their edges (Figure 9d). Additionally, certain quartz grains undergo metasomatic dissolution by clay minerals (Figure 9j).

Fine skeletal particles often fail to provide adequate support for sandstone, leading to sandstone compaction followed by dissolution. This significant constructive diagenesis process faces challenges due to the reduction in pore space and connectivity resulting from compaction. This reduction affects fluid injection, effectively interrupting the interaction between sandstone and the sedimentary environment. Consequently, the entry of hydrocarbons into the sandstone becomes challenging [4,14].

The maximum grain size was not considered in this study due to its distinctive characteristics. Analysis of the four wells in the Zhongqiu section revealed variations in grain size. For instance, the ZQ1 well exhibited poor sorting with significant grain size variability, while the ZQ12 well in Zhongqiu had smaller grain sizes compared to the other wells. These observations suggest minimal changes in grain size within the same statistical range. This consistency also translates into the preservation of primary pore spaces, thanks to the limited fluctuations in grain size relative to the other wells. Preserved pores around larger grains not only contribute to reservoir connectivity but also serve as prerequisites for subsequent fluid–water–rock interactions [14]. Fluid transport through these pores removes reaction products, gradually expanding secondary pores and enhancing pore space, ultimately resulting in favorable pore-enlargement effects [47–49]. Furthermore, the retention of primary pores plays a crucial role in completing diagenesis during the burial process. In contrast, the absence of pores inevitably reduces the incidence of dissolution and subsequent transport of calcium and silica, limiting their modifying effects on the reservoir.

5.3. Prediction of High-Quality Reservoirs

Through an in-depth examination and analysis of core lithology, cast thin sections, scanning electron microscopy, and logging curve data from the Bashijiqike Formation reservoirs in our study area, we conducted a comprehensive assessment of the petrological features, primary reservoir storage space, pore-throat structure, and physical attributes of these reservoirs. Our investigation has led us to conclude that sedimentary microphases play a pivotal role in controlling the distribution of reservoirs, while diagenesis is the principal factor limiting storage space within these reservoirs. Armed with this newfound understanding, we have established a foundational framework for identifying high-quality reservoirs within our study area (Table 2).

Table 2. Reservoir classification criteria for the Zhongqiu field [25,44].

Basis of Division		I	II	III	IV
Physical properties	Porosity Φ (%)	≥12	12~9	9~6	<6
	Permeability K (mD)	≥1.5	1.5~0.5	0.5~0.233	<0.233
Lithologic characters		Coarse siltstone and fine sandstone	Siltstone, fine sandstone, and pebbly sandstone	Limestone siltstone and pebbly sandstone	Muddy, gray siltstone, muddy siltstone, and sandy conglomerates
Plane porosity (%)		>6	6~4	4~1	<1
Pore structure parameter	Displacement pressure Pd (MPa)	<0.5	0.5~1	1~4	>4
	Average throat radius (μm)	>0.4	0.4~0.2	0.2~0.1	<0.1
Pore-throat classification		Medium–small hole and medium–small throat	Small holes and thin throats	Small holes and thin throats	Microporous micro throat
Content of interstitial material (%)		<10	10~15	10~20	>20
Pore characteristics		Remaining primary intergranular pores are predominant, followed by intergranular solution pores; the pores are well connected	Remaining primary intergranular pores are predominant, followed by intergranular soluble pores, with moderate pore connectivity	Intergranular soluble pores, intragranular soluble pores, and medium to poor pore connectivity	Intragranular dissolved pores, heterogeneous matrix pores, and poor pore connectivity
Overall merit		Good	Moderate	Moderate–poor	Non-reservoir
Permeability grading of pores		Low pore permeability	Extra-low pore permeability	Extra-low pore permeability	Dense layer

Utilizing the reservoir classification criteria outlined above, Class I reservoirs are categorized as high-quality reservoirs. In our study area, we have predicted and classified high-quality reservoirs based on their predominant controlling factors, with the findings summarized as follows [50].

High-quality reservoirs within the initial segment of the Bashijiqike Formation predominantly occur in the ZQ1 and ZQ11 wells. In the first subsection of the subsequent section of the Bashijiqike Formation, high-quality reservoirs exhibit the broadest distribution, with the ZQ11 well displaying the highest recorded thickness. For the second subsection of this same section in the Bashijiqike Formation, high-quality reservoirs are categorized into two primary intervals, namely SW and NE. Here, both the ZQ11 and ZQ12 wells exhibit the greatest thickness values. The third subsection of the second section of the Bashijiqike Formation resembles the first section of the Bashijiqike Formation, with the most well-developed high-quality reservoirs occurring in the vicinity of the ZQ11 well (Figure 10). These established classification criteria and outcomes serve as valuable references for assessing and distinguishing large sandstone gas fields.

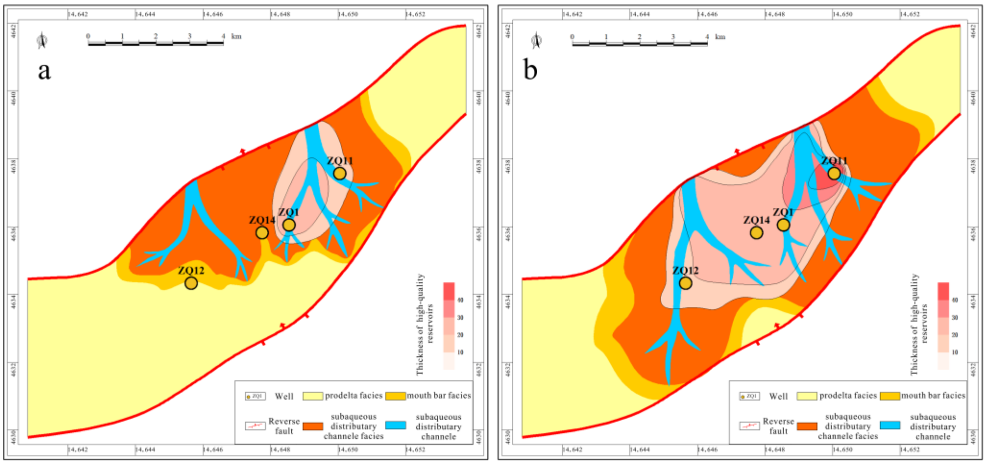

Figure 10. Quality reservoir prediction results. (**a**). K_1bs^1 section high-quality reservoir; (**b**). K_1bs^2 section high-quality reservoir.

6. Conclusions

In this research, we conducted a comprehensive examination of the crucial attributes of the Bashijiqike Formation reservoir in the Zhongqiu field. This investigation encompassed petrological characteristics, mineralogical features, reservoir physical properties, and storage space characteristics. By analyzing the conspicuous distinctions within these features, we scrutinized the principal factors governing the reservoir within the Zhongqiu field. Consequently, our conclusion is that the production disparities in the sandstone-type gas fields at the delta front are closely linked to substrate heterogeneity. Our research findings and conclusions can be summarized as follows:

1. The main factors controlling oil and gas productivity included the variations of petrology, mineralogy, and diagenetic process characteristics. The high content of unstable mineral components and constructive diagenesis could increase reservoir porosity together.
2. Mineral composition indicated the relationship between diagenetic processes and reservoir evolution. The high feldspar content in well ZQ1 corresponded to relatively favorable reservoir properties. The dominant feldspar type was plagioclase, suggesting that early-stage chemical weathering had undergone significant alteration.
3. Sedimentary facies of the Bashijiqike Formation in the Zhongqiu 1 Gas Field played a dominant role in the reservoir distribution. The division of sedimentary facies zones reflects variations in material composition and grain size, serving as the main material basis for reservoirs. Differences in mineral composition can reflect the sedimentary environment of the reservoir.
4. A set of grading criteria for sandstone-type reservoirs in the delta front was established, and the distribution of reservoirs of different grades in different stratigraphic sections varies, with the distribution range of high-quality reservoirs dominated by the range of sedimentary microphases in the subaqueous distributary channel.

The Zhongqiu 1 Gas field represents a substantial sandstone-type whole gas field situated at the delta front, aligning with a significant global archetype of gas fields. Systematic elucidation of the reservoir attributes and distinctions inherent to this category of gas fields, coupled with an investigation into the principal controlling factors, stands to furnish a robust geological foundation for the prospecting and exploitation of analogous gas fields.

Author Contributions: Conceptualization, S.Z. and X.L.; methodology, X.L. and Z.W.; software, Z.W.; validation, Q.D. and C.D.; investigation, S.Z. and X.Y.; resources, S.Z. and Y.W. (Yong Wang); data curation, C.D. and X.Y.; writing, original draft preparation, Z.W. and X.L.; writing, review and editing, Z.W. and S.Z.; visualization, Z.W.; supervision, Y.W. (Yanli Wang) and S.Z.; project administration, S.Z. and Q.D. All authors have read and agreed to the published version of the manuscript.

Funding: This research received no external funding.

Data Availability Statement: Data will be made available upon request.

Acknowledgments: The careful reviews and constructive suggestions of the manuscript by anonymous reviewers are greatly appreciated.

Conflicts of Interest: The authors declare no conflict of interest.

References

1. Zhu, G.Y.; Yang, H.J.; Zhang, B.; Su, J.; Chen, L.; Lu, Y.H.; Liu, X.W. The geological feature and origin of Dina 2 large gas field in Kuqa Depression, Tarim Basin. *Acta Petrol. Sin.* **2012**, *28*, 2479–2492.
2. Xie, H.W.; Luo, H.Y.; Zhang, X.Q.; Duan, Y.J.; Zhang, W.; Xie, Y.N. Structural deformation and petroleum exploration potential of subsalt layer inQiulitage structural belt, Kuqa Depression. *Xinjiang Pet. Geol.* **2020**, *41*, 388–393.
3. Li, J.; Li, J.; Xie, Z.Y.; Wang, H.Z.; Liu, M.C.; Li, D.J.; Ma, W.; Mao, D.F.; Zeng, X. Oil and gas source and accumulation of Zhongqiu 1 trap in Qiulitage structural belt, Tarim Basin, NW China. *Pet. Explor. Dev.* **2020**, *47*, 512–522. [CrossRef]
4. Liu, C.; Xu, Z.P.; Chen, G.; Deng, Y.; Wang, J.P.; Zhao, J.L. Hydrocarbon accumulation conditions and evolution process of the ZQ1 large condensate gas field in the Qiulitage structural belt, Tarim Basin. *Nat. Gas Ind.* **2019**, *39*, 8–17.
5. Li, D.J.; Yi, S.W.; Ran, Q.G.; Liao, W.D.; Song, H.J.; Bai, J.Y. Structural characters and potentiality of the East Qiulitage anticline belt in Kuqa Depression. *Nat. Gas Geosci.* **2016**, *27*, 584–590.
6. Yang, M.; Zhao, Y.M.; Yan, L.; Li, H.H.; Zhang, X.X.; Xu, Z.P.; Luo, H.Y. Structural features of the eastern Qiulitage tectonic belt and petroleum geological significance. *Nat. Gas Geosci.* **2018**, *29*, 826–833.
7. Du, J.H.; Tian, J.; Li, G.X.; Yang, H.J.; Zhang, Y.J.; Li, Y.; Xu, Z.P.; Luo, H.Y. Strategic breakthrough and prospect of Qiulitag structural belt in Kuqa Depression. *China Pet. Explor.* **2019**, *24*, 16–23.
8. Shi, C.Q.; Zhang, H.F.; Zhou, S.Y.; Wang, Z.T.; Jiang, J.; Zhang, X.Q.; Zuo, X.J.; Lou, H.; Wang, Z.H.; Chen, C.C. Comparative study on deep and high yielding reservoir characteristics and controlling factors of Cretaceous Bashijiqike Formation in Kelasu structural belt and Qiulitage structural belt of Kuqa Depression, Tarim Basin. *Nat. Gas Geosci.* **2020**, *31*, 1126–1138.
9. Yi, S.W.; Li, M.P.; Fan, T.Z.; Yang, F.; Fang, H.; Huang, F.X.; Jin, W.D. Exploration directions on the Kelasu and East-Qiulitag fault hanging walls, Kuqa Depression, Tarim Basin. *Oil Gas Geol.* **2021**, *42*, 309–324.
10. Chen, G.; Zhao, J.L.; Yang, X.Z.; Liu, C.; Deng, Y. Characteristics and controlling factors of deep-buried clastic reservoirs in the Qiul-stage structural belt, Tarim Basin. *Nat. Gas Ind.* **2019**, *39*, 18–27.
11. Zhang, X.X.; Tao, X.W.; Yang, M. East akisato tager tectonic belt tectonic characteristics and oil and gas exploration zones. *Geol. Prospect.* **2014**, *50*, 1190–1197.
12. Duan, Y.J.; Luo, H.Y.; Xie, H.W.; Xu, Z.P.; Zhang, X.Q.; Zhang, J.Z.; Shi, L.; Yuan, R. Salt-related structural characteristics and deformation mechanism of Qiulitage structural Belt, Kuqa Depression, Tarim Basin. *Nat. Gas Geosci.* **2021**, *32*, 993–1008.
13. Chang, X.H.; Tian, J.C.; Li, L.; Zhang, X.; Li, R.; Gu, N.; Yang, Z.L. Relationship between lithofacies, logging facies and sand body reservoir in Lower Shihezi Formation of Daniudi Gas Field and its petroleum significance in-plane distribution. *J. Chengdu Univ. Technol. (Sci. Technol. Ed.)* **2013**, *40*, 417–423.
14. Lai, J.; Wang, G.W.; Chai, Y.; Ran, Y.; Zheng, X.H.; Xin, Y.; Zhou, L.; Wu, Q.K. Kuche cretaceous Bashkortostan base of chick strata sequence stratigraphic characteristics. *J. Sediment.* **2015**, *33*, 394–407.
15. Liu, B.J. *Sedimentary Petrology*; Geological Publishing House: Beijing, China, 1980; pp. 15–68.
16. Guo, G.S.; Xing, L.R.; Li, N.; Chen, Z.G. Production characteristics of coalbed methane well group and control factors of productivity difference. *Nat. Gas Geosci.* **2020**, *31*, 1334–1342.
17. Feng, J.W.; Zhao, L.B.; Wang, Y.D. Controlling factors of ultra-deep tight reservoir productivity in Keshen gas field, kuqa depression. *Acta Pet. Sin.* **2020**, *41*, 478–488.
18. Liu, Z.; Zhang, L.; Jiang, K.; Feng, J.Q.; Zhang, T.; Li, Q.Z. Influencing factors of productivity of multi-branch horizontal Wells of coalbed methane and countermeasures to increase and stabilize production: A case study of Sanjiao Block in Ordos Basin. *Nat. Gas Ind.* **2018**, *38*, 65–69.
19. Wang, X.; Liu, C.Z. Analysis of main geological factors controlling single well productivity of Chang 4 + 5 ultra-low permeability reservoir in Jiyuan area. *Miner. Explor.* **2019**, *10*, 584–592.
20. Mei, Y.G.; Lian, X.H.; Zhang, Q.J.; Wang, Q.C.; Guo, J.F.; Shen, X.W.; Zhang, Z. Ooze south Zheng Zhuang block CBM vertical Wells capacity fine resolution. *Control Factors Coal Mine Saf.* **2018**, *49*, 150–154.
21. Wu, Z.X. Main controlling factors of tight gas well productivity in saline gas field. *Unconv. Oil Gas* **2018**, *5*, 62–67.
22. Li, Y.; Fan, A.P.; Yang, R.C.; Sun, Y.P.; Lenhardt, N. Sedimentary facies control on sandstone reservoir properties: A case study from the permian Shanxi Formation in the southern Ordos basin, central China. *Mar. Pet. Geol.* **2021**, *129*, 105083. [CrossRef]
23. Wang, X.L.; Zeng, Q.; Li, R.R.; Wang, Y.F.; Pei, S.Q.; Xin, R.Y. Analysis of controlling factors for high production of tight conglomerate reservoir in the fourth member of xugong formation, zitong sag. *Nat. Gas Technol. Econ.* **2018**, *12*, 19–22+40+81–82.
24. Li, Y.J.; Wang, J.J.; Fan, A.P.; Yang, R.C. Gas east gas well production capacity in the main control factors analysis. *J. Shandong Univ. Sci. Technol. (Nat. Sci. Ed.)* **2010**, *29*, 14–19.

25. Tian, J.C.; Zhang, X.L.; Wang, F.; Chen, R.; Lin, X.B. Quantitative characterization of superposition relationship and distribution of Upper Paleozoic reservoir sand bodies in Gaoqiao Area, Ordos Basin. *Oil Gas Geol.* **2013**, *34*, 737–742+815.
26. Ortiz-Orduz, A.; Ríos-Reyes, C.A.; Vargas-Escudero, M.A.; García-González, M. Impact of diagenesis on the reservoir rock quality of the Cachiri Group tight sandstones in Cesar sub basin (Colombia): A case of study from ANH-CR-MONTECARLO 1X well. *J. Nat. Gas Sci. Eng.* **2021**, *95*, 104138. [CrossRef]
27. Oluwadebi, A.G.; Taylor, K.G.; Dowey, P.J. Diagenetic controls on the reservoir quality of the tight gas Collyhurst Sandstone Formation, Lower Permian, East Irish Sea Basin, United Kingdom. *Sediment. Geol.* **2018**, *371*, 55–74. [CrossRef]
28. Khazaie, E.; Noorian, Y.; Kavianpour, M.; Moussavi-Harami, R.; Mahboubi, A.; Omidpour, A. Sedimentological and diagenetic impacts on porosity systems and reservoir heterogeneities of the Oligo-Miocene mixed siliciclastic and carbonate Asmari reservoir in the Mansuri oilfield, SW Iran. *J. Pet. Sci. Eng.* **2022**, *213*, 110435. [CrossRef]
29. Zhang, Q.; Liu, R.H.; Pang, Z.L.; Lin, W.; Bai, W.H.; Wang, H.Y. Characterization of microscopic pore structures in Lower Silurian black shale(S1l), southeastern Chongqing, China. *Mar. Pet. Geol.* **2016**, *71*, 250–259. [CrossRef]
30. Farahani, M.; Aghaei, H.; Masoumi, H. Effect of pore type on porosity, permeability and pore volume compressibility of geological formations due to in-situ stress change. *J. Pet. Sci. Eng.* **2022**, *218*, 110986. [CrossRef]
31. Zeng, Q.L.; Mo, T.; Zhao, J.L.; Tang, Y.L.; Xia, J.F.; Hu, C.L.; Shi, L.L. Characteristics, genetic mechanism and oil & gas exploration significance of high-quality sandstone reservoirs deeper than 7000 m: A case study of the Bashijiqike Formation of Lower Cretaceous in the Kuqa epression, NW China. *Nat. Gas Ind. B* **2020**, *7*, 317–327.
32. Vaisblat, N.; Harris, B.H.; Ayranci, K.; Chalaturnyk, R.; Power, M.; Twemlow, C.; Minion, N. Petrophysical properties of a siltstone reservoir—An example from the Montney Formation, western Canada. *Mar. Pet. Geol.* **2022**, *136*, 105431. [CrossRef]
33. Li, G.Y.; Lai, F.Q.; He, J.C.; Tang, L.; Hu, J. Characteristics and main controlling factors of physical properties of Lower Jurassic tight sandstone reservoirs in Qiudong Subsag, Turpan-Hami Basin. *Nat. Gas Geosci.* **2013**, *24*, 310–319.
34. Li, J.F.; Yang, L.R.; Zhang, F.B.; Luo, J.Y.; Xue, Q.; Cao, D.D.; Zhang, X.W.; Wu, D. The main controlling factors and 'sweet spot' model of tight oil enrichment in Chang 8 Member of Yanchang Formation in Xiasiwan Oilfield. *Oil Gas Field Eval. Dev.* **2019**, *9*, 1–9.
35. Zhao, M.S.; Tian, J.C.; Zhang, X.; Su, B.R. Analysis of reservoir characteristics and its main controlling factors-Taking the Lower Permian Shanxi Formation in the Shilijiahan area of northern Hubei as an example. *Fault Block Oil Gas Fields* **2020**, *27*, 155–159.
36. Liu, J.T.; Wang, J.S.; Ren, Z.Y.; Zhang, H.; Wang, X.G. Hydrocarbon accumulation characteristics and main controlling factors of Xishanyao Formation in Xiaocaohu subsag. *Spec. Reserv.* **2014**, *21*, 10–14+141.
37. Zhou, X.H.; Wang, D.Y.; Yu, H.B.; Yang, H.F.; Li, L. Major controlling factors and hydrocarbon accumulation models of large-scale lithologic reservoirs in shallow strata around the Bozhong sag, Bohai Bay Basin, China. *Pet. Explor. Dev.* **2022**, *49*, 660–669+740. [CrossRef]
38. Zhao, W.Z.; Wang, H.J.; Xu, C.C.; Bian, C.S.; Wang, Z.C.; Gao, X.H. Reservoir-forming mechanism and enrichment conditions of the extensive Xujiahe Formation gas fields, central Sichuan Basin. *Pet. Explor. Dev.* **2010**, *37*, 146–157.
39. Qiu, X.L.; Chen, X.D.; Ding, L.; Tan, Y.H.; Huang, Q. The structural characteristics of the sand body of the Chang 8_1 oil layer group in the Jiyuan area and its control on the reservoir. *Geol. Sci. Technol. Bull.* **2020**, *39*, 87–96.
40. Room, S.A.e.; Chen, Z.; Ullah, H.; Ahmad, W.; Ali, M. Reservoir characteristics and controlling factors of Permian glutenite in Northern Zhongghai uplift, Junggar Basin, China. *Ore Energy Resour. Geol.* **2023**, *15*, 100025. [CrossRef]
41. Li, H.P.; Wu, Y.; Liu, R.M. Difference and accumulation model of oil and gas accumulation in Dabei structural belt of Kuqa depression. *Pet. Geol. Eng.* **2021**, *35*, 25–30.
42. Xiao, L.; Yang, L.; Zhang, X.; Guan, X.; Wei, Q. Densification Mechanisms and Pore Evolution Analysis of a Tight Reservoir: A Case Study of Shan-1 Member of Upper Paleozoic Shanxi Formation in SW Ordos Basin, China. *Minerals* **2023**, *13*, 960. [CrossRef]
43. Zhou, L.; Li, Y.; Jin, F.; Fu, L.; Pu, X.; Da, L.; Li, H.; Liu, H.; Xu, W. Tight Sandstone Reservoir Formation Mechanism of Upper Paleozoic Buried Hills in the Huanghua Depression, Bohai Bay Basin, Eastern China. *Minerals* **2021**, *11*, 1368. [CrossRef]
44. Zhao, G.; Li, X.; Liu, M.; Dong, C.; Chen, D.; Zhang, J. Reservoir Characteristics of Tight Sandstone and Sweet Spot Prediction of Dibei Gas Field in Eastern Kuqa Depression, Northwest China. *Energies* **2022**, *15*, 3135. [CrossRef]
45. Al-Juboury, A.; Howard, J.P.; Vincent, S.J.; Nichols, G. Petrography, diagenesis and geochemistry of the Cambro-Ordovician Khabour sandstones, western Iraq: Implications for reservoir quality and the impact of the Hirnantian glaciation. *Mar. Pet. Geol.* **2021**, *123*, 104733. [CrossRef]
46. Lanz, M.D.R.; Azmy, K.; Cesaretti, N.N.; Fortunatti, N.B. Diagenesis of the Vaca Muerta Formation, Neuquén Basin: Evidence from petrography, microthermometry and geochemistry. *Mar. Pet. Geol.* **2021**, *124*, 104769. [CrossRef]
47. Moyano-Paz, D.; Gómez-Dacal, A.R.; Varela, A.N.; Comerio, M.; Muñoz-Olivero, T.M.; Bucher, J.; Richiano, S.; Poiré, D.G. Controls on composition and diagenesis of wave- and river-dominated deltas: Impacts on reservoir properties. An example from the La Anita Formation (Argentina). *Mar. Pet. Geol.* **2022**, *138*, 105571. [CrossRef]
48. Li, W.; Fan, T.; Gao, Z.; Wu, Z.; Li, Y.; Zhang, X.; Zhang, H.; Cao, F. Impact of Diagenesis on the Low Permeability Sandstone Reservoir: Case Study of the Lower Jurassic Reservoir in the Niudong Area, Northern Margin of Qaidam Basin. *Minerals* **2021**, *11*, 453. [CrossRef]

49. Umar, M.; Friis, H.; Khan, A.S.; Kassi, A.M.; Kasi, A.K. The effects of diagenesis on the reservoir characters in sandstones of the Late Cretaceous Pab Formation, Kirthar Fold Belt, southern Pakistan. *J. Asian Earth Sci.* **2011**, *40*, 62. [CrossRef]
50. Xu, X.; Liu, L.Y.; Li, X.J.; Yang, W.J.; Cao, Y.G.; Ma, H.; He, A.A.; Wang, R.Y.; Leng, H.B.; Zhu, Y.S.; et al. Sequence stratigraphy, sedimentary characteristics of barrier coastal sedimentary system of the Benxi Formation (Gaoqiao area, Ordos basin) and favorable reservoir distribution. *Energy Rep.* **2021**, *7*, 5316–5329. [CrossRef]

Disclaimer/Publisher's Note: The statements, opinions and data contained in all publications are solely those of the individual author(s) and contributor(s) and not of MDPI and/or the editor(s). MDPI and/or the editor(s) disclaim responsibility for any injury to people or property resulting from any ideas, methods, instructions or products referred to in the content.